**ORIGINAL ARTICLE**

# Engineering CRISPR/Cpf1 with tRNA promotes genome editing capability in mammalian systems

Han Wu[1,2,3] · Qishuai Liu[1,2,3] · Hui Shi[1,2,3] · Jingke Xie[1,2,3] · Quanjun Zhang[1,3] · Zhen Ouyang[1,3] · Nan Li[1,2,3] · Yi Yang[5] · Zhaoming Liu[1,3] · Yu Zhao[1,3] · Chengdan Lai[1,3] · Degong Ruan[1,2,3] · Jiangyun Peng[1,2,3] · Weikai Ge[1,2,3] · Fangbing Chen[1,2,3] · Nana Fan[1,3] · Qin Jin[1,2,3] · Yanhui Liang[1,2,3] · Ting Lan[1,2,3] · Xiaoyu Yang[1,6] · Xiaoshan Wang[1,2,3] · Zhiyong Lei[7,8] · Pieter A. Doevendans[7,8] · Joost P. G. Sluijter[7,8] · Kepin Wang[1,3] · Xiaoping Li[1,3] · Liangxue Lai[1,3,4]

## Abstract

CRISPR/Cpf1 features a number of properties that are distinct from CRISPR/Cas9 and provides an excellent alternative to Cas9 for genome editing. To date, genome engineering by CRISPR/Cpf1 has been reported only in human cells and mouse embryos of mammalian systems and its efficiency is ultimately lower than that of Cas9 proteins from *Streptococcus pyogenes*. The application of CRISPR/Cpf1 for targeted mutagenesis in other animal models has not been successfully verified. In this study, we designed and optimized a guide RNA (gRNA) transcription system by inserting a transfer RNA precursor (pre-tRNA) sequence downstream of the gRNA for Cpf1, protecting gRNA from immediate digestion by 3′-to-5′ exonucleases. Using this new gRNA[tRNA] system, genome editing, including indels, large fragment deletion and precise point mutation, was induced in mammalian systems, showing significantly higher efficiency than the original Cpf1-gRNA system. With this system, gene-modified rabbits and pigs were generated by embryo injection or somatic cell nuclear transfer (SCNT) with an efficiency comparable to that of the Cas9 gRNA system. These results demonstrated that this refined gRNA[tRNA] system can boost the targeting capability of CRISPR/Cpf1 toolkits.

**Keywords** CRISPR/Cpf1 · gRNA[tRNA] system · Genome editing · Rabbit · Pig

---

Han Wu, Qishuai Liu contributed equally to this work.

✉ Kepin Wang
wang_kepin@gibh.ac.cn

✉ Xiaoping Li
li_xiaoping@gibh.ac.cn

✉ Liangxue Lai
lai_liangxue@gibh.ac.cn

1 CAS Key Laboratory of Regenerative Biology, Joint School of Life Sciences, Guangzhou Institutes of Biomedicine and Health, Guangzhou Medical University, Chinese Academy of Sciences, Guangzhou 510530, China

2 University of Chinese Academy of Sciences, Beijing 100049, China

3 Guangdong Provincial Key Laboratory of Stem Cell and Regenerative Medicine, South China Institute for Stem Cell Biology and Regenerative Medicine, Guangzhou Institutes of Biomedicine and Health, Chinese Academy of Sciences, Guangzhou 510530, China

4 Jilin Provincial Key Laboratory of Animal Embryo Engineering, Institute of Zoonosis, College of Veterinary Medicine, Jilin University, Changchun 130062, China

5 Key Laboratory for Major Obstetric Diseases of Guangdong Province, Key Laboratory of Reproduction and Genetics of Guangdong Higher Education Institutes, The Third Affiliated Hospital of Guangzhou Medical University, Guangzhou 510150, China

6 Institute of Physical Science and Information Technology, Anhui University, Hefei 230601, China

7 Department of Cardiology, Experimental Cardiology Laboratory, University Medical Center Utrecht, 3584CX Utrecht, The Netherlands

8 Netherlands Heart Institute, 3584CX Utrecht, The Netherlands

## Introduction

CRISPR/Cas9 system has emerged as a revolutionized technique for genomic engineering in both prokaryotic and eukaryotic organisms [1]. Cas9 protein is an RNA-guided endonuclease that functions with single guide RNA (gRNA) [2, 3]. The widely used Cas9 from Streptococcus pyogenes (SpCas9) prefers a guanidine-rich, NGG protospacer adjacent motif (PAM) sequence which limits the selection of target sites. As a result, targeting double-stranded breaks (DSBs) with the precision necessary for various genome editing applications can often be difficult. In addition, the off-targeting effect of gene editing is a significant concern for clinical applications of SpCas9. Lately, much effort has been exerted to engineer Cas9 orthologs and variants with purposefully altered PAM specificities and reduce off-targeting effects. Several altered PAM specificity variants enable the robust editing of endogenous gene sites not targetable by wild-type (WT) SpCas9, and their genome-wide specificities are comparable to that of WT SpCas9. These Cas9 orthologs and engineered Cas9 variants can recognize other PAM sequences and have expanded the set of available target sites [4, 5].

Recently, a new RNA-guided endonuclease, Cpf1 [6] was identified and harnessed for editing the genomes of plants (rice [7–9], tobacco [7, 10], *Arabidopsis* [9] and soybean [10]), bacteria [11], *Drosophila* [12], mice [13–17], and human cells [18–21]. In contrast to Cas9, Cpf1 recognizes a thymidine-rich PAM (5′-TTTN-3′) sequence at the 5′ end of the target DNA sequence, aiding in targeting regulatory regions or AT-rich genomes, and complements the CRISPR/Cas9 system (5′-NGG-3′ PAM). In addition, Cpf1 is guided by a single, short crRNA transcript (~ 40–43 nt) [6], which is less than half of the length of Cas9 (~ 80–100 nt). Unlike Cas9, which generates cleavage products with blunt ends within the PAM-proximal target site, Cpf1 creates staggered ends with three- to five-nucleotide 5′ overhangs distal to the PAM site [6, 22]. This condition may facilitate the precision of gene modification mediated by non-homologous end joining (NHEJ) [23]. Cpf1 nucleases have also been shown to exert lower off-target effects than Cas9 nucleases [18, 19], thus presenting significant potential for clinical applications [17]. Overall, these unique features of CRISPR/Cpf1 have shown that this system is a potentially better genome editing tool than the CRISPR/Cas9 system. Three groups have recently reported that mutant mice can be generated using preassembled recombinant CRISPR/Cpf1 ribonucleoproteins [13] or mRNA–gRNA mixtures [14], but the targeting rates were lower than those of SpCas9. Watkins-Chow et al. observed that Cpf1 activity in mouse zygotes was highly dependent on RNA concentration [15] and that an RNA concentration that was effective for Cas9 was ineffective for Cpf1. The application of a high concentration of RNA may negatively affect embryo and cell survival and growth. This phenomenon may explain why the potential of Cpf1 for targeted mutagenesis in other animal models has not been successfully verified.

Inspired by the tRNA boosting, the CRISPR/Cas9 editing capability, here we optimized a Cpf1-gRNA^tRNA expression system by adding a pre-tRNA sequence in the downstream of Cpf1-crRNA to enhance the CRISPR/Cpf1-mediated genome editing. Taking the advance of the refined Cpf1-gRNA^tRNA system, we have achieved robust targeting efficiency in mammalian cells (human cell lines and porcine fetal fibroblasts (PFFs)) and embryos (rabbit zygotes and porcine parthenogenetic embryos). Moreover, we achieved the *WRN* gene knockout (KO) rabbits with Werner syndrome by direct injection of Cpf1 mRNA and gRNA^tRNA into zygotes followed by transfer into synchronized recipients [24]. Furthermore, *dystrophin* (*DMD*) gene-KO pigs and *PLN*^*R14del* point mutation pigs were also generated by combining Cpf1-gRNA^tRNA-mediated fibroblast mutation and somatic cell nuclear transfer (SCNT) [25, 26].

## Materials and methods

### Animals

All procedures of animal experiment facilities were approved by the Department of Science and Technology of Guangdong Province (ID SYXK 2005-0063). Surgical procedures were performed under anesthesia in accordance with the guidelines of Institutional Animal Care and Use Committee (IACUC) of Guangzhou Institutes of Biomedicine and Health (GIBH), Chinese Academy of Sciences (Animal Welfare Assurance #A5748-01), and all efforts were exerted to minimize animal suffering.

### Vector construction

Human codon-optimized AsCpf1 protein with double SV40 NLS was synthesized and sub-cloned into pcDNA3.1 and pCS2 plasmids. To construct the AsCpf1 gRNA cloning plasmid, the gRNA^tRNA fragment with two BpiI restriction sites was amplified by PCR using specific primers and cloned into a pMD18-T (Takara) vector. Based on the presence of the TTTV PAM region, AsCpf1 guide RNA was designed in the early exon, and a 20–24 bp protospacer following the PAM was selected as a target site. Two complementary oligo DNA containing target sequences and 4-bp overhangs were synthesized and annealed by boiling for 10 min, cooled to room temperature, ligated into

a BpiI-digested gRNA cloning vector, and confirmed by Sanger sequence analysis (IGE, Guangzhou, China).

## In vitro transcription

The pCS2-AsCpf1 plasmid was linearized with NotI and purified with QiAquick PCR Purification Kit. Then, mRNA was transcribed using the mMessage mMachine SP6 Kit (Thermo Fisher/Ambion). RNA was recovered using the Rneasy MinElute Cleanup kit and stored in aliquots at $-80$ °C.

We compared two different types of gRNA structure. One was a gRNA$^{tRNA}$ type, and the other included an original gRNA. For gRNA$^{tRNA}$, a custom target site was first cloned into the gRNA expression plasmid. Then, we amplified the gRNA$^{tRNA}$ region with primer pairs: F1, 5′-CTAATA CGACTCACTATAGGTAATTTCTACTCTTGTAG-3′; R1, 5′-TAAAAAAAATGCACCAGCCG-3′. For the original type, pairs of oligonucleotides containing a T7 promoter, crRNA, and target sequences were synthesized, denatured, cooled down, and then cloned into the pMD18-T vector. The correct plasmid was used as a template to amplify the sequence for in vitro RNA transcription with primers pairs: F2, 5′-GCTTGCATGCCTGCAGGTCG-3′; R2, 5′-TGATTA CGAATTCGAGCTCG-3′. PCR products amplified from two types of gRNA were used as a template for in vitro RNA synthesis with a T7 High Yield RNA Synthesis Kit (NEB E2040S).

The quality of the synthesized RNA was analyzed by 1% agarose gel electrophoresis at 170 V for 4 min and its concentration was determined by spectrophotometry. All reagents used in the experiments mentioned above were RNase-free.

## Pig and rabbit embryo injection

Pig parthenogenetic embryos were cultured following a previous protocol [27]. The AsCpf1 mRNA and gRNA mixture was microinjected after activation for 1 h. Six days after injection, morula or blastocyst stage embryos were collected individually and lysed with NP40 solution. The lysate was used as a template for PCR. Then, Sanger sequencing was performed to preliminarily determine the mutation. PCR products showing different curves were compared with those of the WT genome.

As for rabbits, donor rabbits were performed following published procedures [24]. Rabbit zygotes were collected from donor rabbits, and 50 ng/μL AsCpf1 mRNA and 20 ng/μL gRNA were mixed well and injected into rabbit one-cell stage zygotes. Then, the injected zygotes were transferred into the oviducts through the fimbriae, leaving 30 zygotes cultures in vitro. Morula or blastocyst stage embryos were individually collected and lysed with NP40 solution.

Subsequently, PCR amplification of the sequence around the target site was performed with Sanger sequencing.

## PFFs culture, transfection, and selection

PFFs were isolated from 35-day-old fetuses of Bama miniature pig from Chongqing. The fetuses, removed heads, tails, limbs, and viscera were digested in cell culture medium containing 0.32 mg/mL collagenase IV and 2500 IU/mL DNase I for 3 h at 39 °C. Isolated PFFs were then cultured in 10-cm dishes for 12 h and frozen in fetal bovine serum containing 10% dimethylsulfoxide. A day before transfection, PFFs were thawed and cultured in 10-cm dishes until 90% confluency. Approximately $2 \times 10^6$ cells were electroporated using Neon transfection system (Life Technology) at 1350 V, 30 ms, and 1 pulse in 100 μL of Buffer B containing AsCpf1 and *DMD*-gRNA$^{tRNA}$ or *PLN*-gRNA$^{tRNA}$ expression plasmids (*PLN* including the ssODN as donors). Electroporated cells were transferred into 20 culture dishes at 500 cells/10 mL. After a 48-h recovery, 1 mg/mL G418 (Merck) was added to the cell culture. After a 10–14-day selection, colonies were retrieved and cultured in 24-well plates using cloning cylinders.

Cells normally reached confluency in $3 - 5$ days and were then trypsinized and suspended in 1 mL of culture media. A total of 600 μL cells ($0.6 \times 10^5$ cells) were plated in 24-well plates, and the remaining cells were used to extract DNA for PCR screening. PCR screening primers were as follows: *DMD*-F:5′-GACTGCAACACTCTAGGAAAGC-3′ and *DMD*-R: 5′-GTGCAAGACACACTGTGCTTGG-3′; *PLN*-F: 5′-CTGAGAGAAGGAGGCAAGAACT-3′, and *PLN*-R: 5′-AGAACTTCTGCTGAGGAAGTGG-3′. The PCR condition was 95 °C for 5 min; 98 °C for 10 s, 68 °C for 30 s ($-0.6$ °C/cycle), 72 °C for 1 min, for 35 cycles; 72 °C for 5 min; and held at 12 °C. PCR products were sequenced to detect mutations. Some PCR products were selected to ligate into a pMD18-T vector (Takara, Dalian, China) and sequenced to determine exact mutant sequences. Positive cell colonies were expanded and then cryopreserved. These cells were thawed and cultured to reach sub-confluency in a 24- or 12-well plate before SCNT.

## SCNT and production of mutant pigs

Porcine oocytes were collected from a local slaughter house and transported to the laboratory. Maturate oocytes were enucleated by aspirating the first polar body and adjacent cytoplasm with a glass pipette in a manipulation medium of HEPES-buffered M199 plus cytochalasin B (7.5 μg/mL). The cells identified as biallelic KO by gene sequencing were thawed and used as donor cells to be injected into the perivitelline space of oocytes. Fusion and activation were performed with two successive DC pulses at 1.2 kV/cm

for 30 μs using an electrofusion instrument. Reconstructed embryos were kept in manipulation medium without cytochalasin B for 30 min, and fusion rate was evaluated. After a 20-h culture in embryo-development medium PZM3 at 39 °C, reconstructed embryos were surgically transferred into the oviduct of a surrogate the day after estrus was observed. Once detected, pregnancy status was monitored weekly until delivery. The cloned piglets were delivered by natural birth. Genomic DNA isolated from ear skin biopsy of the newborn cloned piglets was used for PCR genotyping, and fibroblasts were isolated and cultured by methods similar to PFFs.

## Genotype identification

Genomic DNA was extracted from newborn pigs and rabbit ear tissues using TIANamp Genomic DNA kit (Tiangen). PCR productS spanning target sites of approximately 500–700 bp were generated. Then, Sanger sequencing was performed. For piglet, it comes from SCNT, and genotype is clear. PCR primers for rabbits were follows: rWRN-E4F: 5′-GAAGTGGAACAGCTGGGACTTG-3′; rWRN-E4R: 5′-ACCTCACAGGGTGTTACGAA-3′; rWRN-E6F: 5′-AAT GCAGCTCTTGTGTCTTGC-3′; rWRN-E6R: 5′-TCTGTT GAATGGCACTCGCT-3′. The PCR condition was 95 °C for 5 min; 98 °C for 10 s, 58 °C for 30 s, 72 °C for 50 s, for 35 cycles, 72 °C for 5 min; and held at 12 °C. PCR products were evaluated by Sanger sequencing. However, most rabbits presented mosaic genotype patterns, and PCR products were ligated to the pMD18-T vector and sequenced with the M13 primer.

## RNA extraction and RT-PCR analysis

To perform RT-PCR, total mRNAs were extracted from porcine hearts using TRIzol Reagent (Life Technology). cDNAs were synthesized using a FastQuant RT Kit (Tiangen). The primers used to amplify *PLN*-cDNA were: F, 5′-CATAAA CAGCCAAGGCTGCCTA-3′; R: 5′-CTTCTGCTGAGG AAGTGGTCTC-3′. The porcine glyceraldehyde-3-phosphate dehydrogenase (GAPDH) gene was used as the control (F, 5′-GATGGCCCCTCTGGGAAACTGTG-3′ and 5′-GGA CGCCTGCTTCACCACCTTCT-3′). The RT-PCR product was predicted to be 380 bp and was sequenced by IGE.

## Western blotting

For Western blotting, biceps femoris muscle, heart and diaphragm tissues of *DMD* KO and age-matched WT piglets were lysed in lysis buffer (10% glycerol, 10% 2-mercaptoethanol, 0.5 M Tris–HCl, and 1% sodium dodecyl sulfate). Total proteins were separated in 7.5% SDS–PAGE gels and transferred to PVDF membranes (Millipore). Membranes were probed with specific primary antibodies and then incubated with HRP-conjugated secondary antibodies. The signal was visualized using ECL plus (Amersham) in accordance with the manufacturer's instructions. Detailed information is provided in our previous reports [28].

## Histological and immunofluorescence staining

The collected tissues (biceps femoris muscle, heart, and diaphragm muscle) from the cloned and age-matched WT piglets were fixed in 4% paraformaldehyde for 2 days. The fixed tissues were then dissected, embedded in paraffin wax, and then cross-sectioned at 3 μm for slides for hematoxylin–eosin (H&E) staining and immunofluorescence (IF) analyses. H&E staining was performed as previously described [25]. For IF staining, antigen was retrieved in 1 M citrate buffer (pH 6.0) for 20 min. The treated tissues were then immunostained with primary antibodies to porcine dystrophin protein and visualized using an Alexa Fluor 594–conjugated goat anti-rabbit IgG secondary antibody. Images of micrographs were taken using a Zeiss microscope (Axiovert 200 MOT).

## Off-target analysis

To analyze potential off-target events in gene-modified rabbits and piglets, off-target sites containing $3 - 5$ mismatches were selected using Cas-OFFinder (http://www.rgenome.net/cas-offinder/) [29]. Genomic DNAs extracted from these rabbits and piglets were used as templates to amplify DNA fragments containing the putative off-target sites by PCR with specific primers. The PCR products were approximately 170-200 bp and were used for library construction. Equal amounts of PCR amplicons were mixed and subjected to deep sequencing on an Illumina MiSeq System.

# Results

## Design and optimization of the Cpf1-gRNA^tRNA gene editing system

An engineered Cpf1-gRNA^tRNA system was established by insertion of the pre-tRNA sequence with a length of 70–80 bp into a position after the target sequence (20–24 bp) of the original gRNA for Cpf1. The total length of Cpf1-gRNA^tRNA was measured as 120–130 bp, and this range is similar to that of Cas9 gRNA (approximately 110 bp) (Fig. 1a, b).

To screen the most suitable pre-tRNA that results in the highest gene editing efficiency in mammal cells and embryos, we defined 43 different pre-tRNA decoding 20 standard amino acids among 597 pre-tRNAs based on
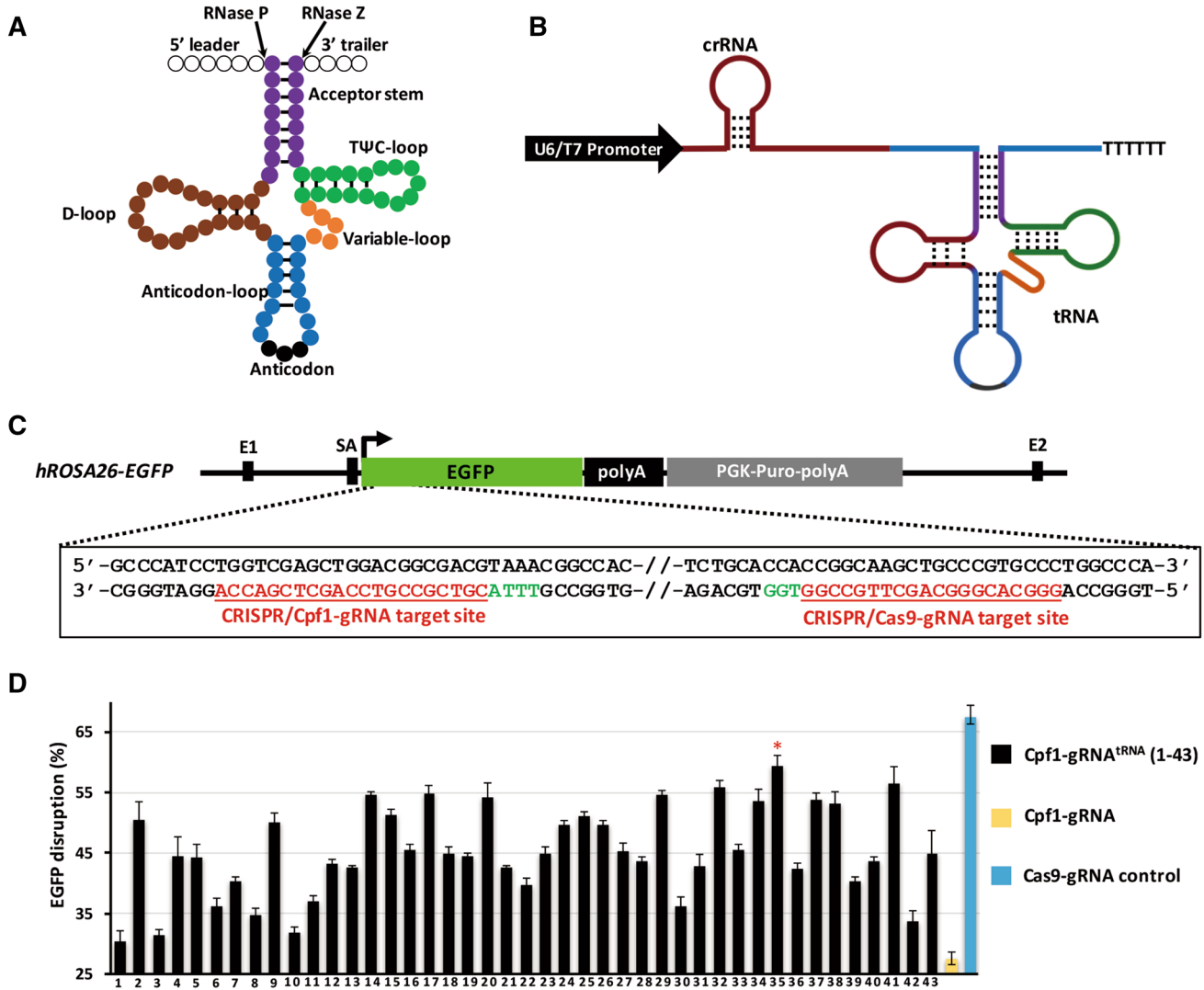
**Fig. 1** Design and optimization of the Cpf1-gRNA^tRNA expression structure. **a** Secondary cloverleaf structure of the eukaryotic pre-tRNA. Acceptor stem is colored in purple, variable loop in orange, D arm in brown, T arm in green, anticodon-loop in blue, anticodon in black, 5′ leader and 3′ tailor in blank circles. This pre-tRNA can be cleaved by RNase P and RNase Z at specific sites. **b** Structure of Cpf1 gRNA^tRNA system with U6/T7 promoter-gRNA-tRNA. **c** One gRNA for Cas9 and one gRNA for Cpf1 were designed and assembled to target the *hROSA26-EGFP* (green highlight). Red letters indicate the sequence of target site, and green letters indicate the PAM site. **d** EGFP disruption rates of 43 different gRNA^tRNA with Cpf1 shows that pre-tRNA^{Gln−TTG−1−1} featured the highest gene editing efficiency

the predicted score in the human genomic tRNA database (http://gtrnadb.ucsc.edu/) (Table S1). 43 pre-tRNAs were individually added to the gRNA for Cpf1 to target enhanced green fluorescent protein (EGFP) (Fig. 1c).

To facilitate evaluation of the genome editing efficiency of the gRNA^tRNA gene editing system, we established a human embryonic kidney 293 (HEK293) cell line with a fluorescence reporter (human ROSA26 (*hROSA26*)-EGFP) wherein a single copy of the EGFP-coding sequence was inserted into one allele of the *hROSA26* locus via homologous recombination. The expression of EGFP driven by endogenous *hROSA26* promoter was very high and stable (Fig. 1c, Fig. S1a–1d). EGFP-Cpf1-gRNA flanked with 43

different human pre-tRNA sequences was individually co-transfected with AsCpf1 into *hROSA26*-EGFP cell lines. The Cas9 gRNA system and original Cpf1-gRNA targeting the early sequence of EGFP were used as the control (Fig. 1c). Seven days' post-transfection, flow cytometry analysis was performed to determine the gene editing efficiency. As shown in Fig. 1d, the gene editing efficiency of the original Cpf1-gRNA reached 26.57%, whereas the gene editing efficiency of Cpf1-gRNA^tRNAs ranged from 30.40 to 59.37% with different pre-tRNAs. The tRNA^{Gln−TTG−1−1} given the highest efficiency 60%, which is close to that of the CRISPR/Cas9 control (67.33%). Therefore, crRNA flanked with pre-tRNA^{Gln−TTG−1−1}, named Cpf1-gRNA^tRNA, was

**Fig. 2** Optimized Cpf1-gRNA$^{tRNA}$ system facilitates efficient genome editing in mammal cells and embryos. **a** Sequence and predicted secondary structure of Cpf1-gRNA$^{tRNA}$. **b** Target sites of three different human endogenous genes of *AAVS1*, *Tet1* and *Tet2*. For *AAVS1* and *Tet2*, we designed five and four corresponding gRNAs of sense sequences, respectively. For *Tet1*, two gRNAs were in the sense sequences, and the other two gRNAs were in the antisense sequence. **c**, **d** Modification percentage rate of endogenous genes (*AAVS1*, *Tet1*, and *Tet2*) induced by gRNA$^{tRNA}$ and gRNA system at 13 gene sites of the HEK293 cells (left panel, determined by T7E1 assay) and Hela cells (right panel). Error bars, s.e.m.; $n = 3$. **e** Blastocyst rates of PA porcine embryos injected with Cpf1 mRNA and gRNAs targeting *NLRP3, ROSA26, APP,* and *GGTA1* loci with gRNA$^{tRNA}$ or gRNA structure. **f** Modified rates of porcine blastocyst injected with mRNAs of Cpf1-gRNA$^{tRNA}$ or Cpf1-gRNA system targeting early exons of *NLRP3, ROSA26, APP,* and *GGTA1* loci

used to perform gene editing in mammalian genomes in the following experiments (Fig. 2a).

Previous studies have reported that AsCpf1 is highly specific with substantially fewer off-target cleavage sites than Cas9. We then verified whether increased efficiency would affect targeting specificity by inserting pre-tRNA into Cpf1-gRNA. To achieve this purpose, we first created variant targeting sequences for EGFP in Cpf1-gRNA$^{tRNA}$ harboring one or two mismatches in positions 1–21 (numbered 1 to 21 in the 5′ to 3′ direction) (Fig. S3). The vector of Cpf1-gRNA$^{tRNA}$ with variant mismatched targeting sequences was individually transfected into *hROSA26*-EGFP cells with a Cpf1 expression plasmid. Seven days'

post-transfection, flow cytometry analysis was performed to test the ratio of cells without green fluorescence, representing the disrupting efficiency of the EGFP gene. As shown in Fig. S3, EGFP disruption was observed by single mismatches of the targeting sequence at most positions of the EGFP-gRNA$^{tRNA}$, whereas two mismatches in the adjacent and separated positions at positions 1–18 resulted in almost complete loss of Cpf1 activity. Two adjacent mismatches of the PAM-distal bases between positions 19 and 21 presented substantially less pronounced effects on the mutagenic activities of Cpf1 nucleases EGFP-gRNA$^{tRNA}$. These results indicated that EGFP-gRNA$^{tRNA}$ maintained high gene-targeting specificity (similar to that of original

Cpf1-gRNA in human cells), although it can tolerate mismatches at the PAM-distal end.

We also examined whether the gene editing efficiency of EGFP-gRNA$^{tRNA}$ was associated with the length of the targeting sequence. We observed that EGFP-gRNA$^{tRNA}$ required at least 18nt of target sequence to achieve efficient DNA cleavage in human cells (Fig. S4a–b). These results were similar to those demonstrated for FnCpf1, wherein DNA cleavage requires a minimum of 18nt of spacer sequence [6].

## Genome editing efficiency of endogenous genes in human cells and mammalian embryos using the Cpf1-gRNA$^{tRNA}$ system

To firmly validate the gene editing efficiency of the Cpf1-gRNA$^{tRNA}$ system, human endogenous genes were targeted by the engineered Cpf1-gRNA$^{tRNA}$ system. We selected 21–24nt target sequences to induce mutations at 13 sites of three different human endogenous genes, i.e., *Tet methylcytosine dioxygenase 1* (*TET1*), *Tet methylcytosine dioxygenase 2* (*TET2*), and *adeno-associated virus integration site 1* (*AAVS1*) (Fig. 2b, Fig. S5a–b). HEK293 and HeLa cells were electroporated with plasmids encoding AsCpf1 and gRNA$^{tRNA}$ or original gRNA, respectively. Three days' post-electroporation, genomic DNA was extracted and purified polymerase chain reaction (PCR) products corresponding to the amplified targeted sites were digested with T7 endonuclease I. As shown in Fig. 2c and d, Cpf1-gRNA$^{tRNA}$ resulted in cleavage efficiency values ranging from 8.7 to 68.3% in HEK293 cells and 5.5 to 66.1% in HeLa cells in the 13 target sites of the three genes, whereas the original Cpf1-gRNA achieved lower efficiencies, ranging from 4.2 to 45.0% in HEK293 cells and 2.2 to 42.7% in HeLa cells.
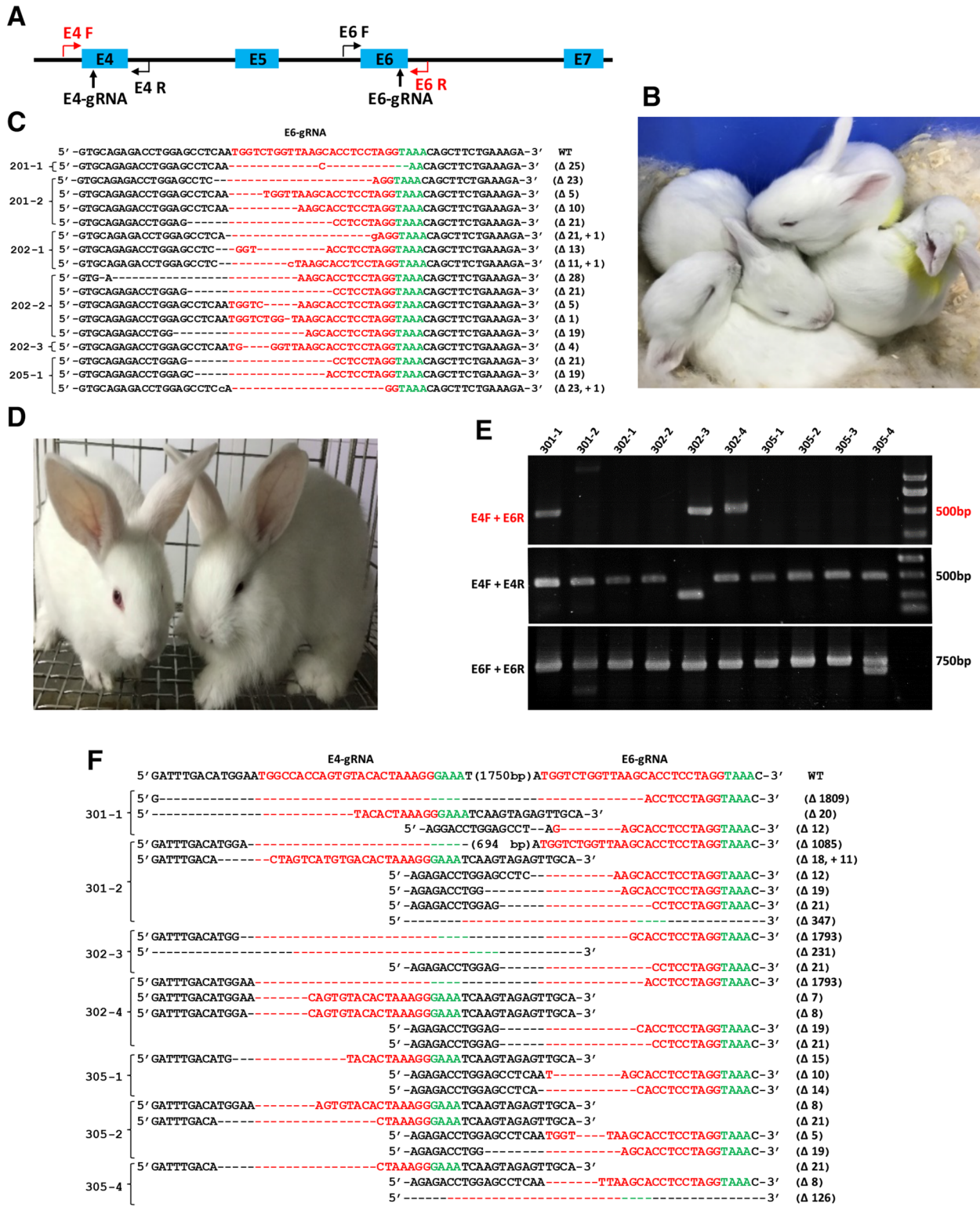
Subsequently, we investigated whether the gRNA$^{tRNA}$ system can enhance targeting efficiency in mammal embryos similar to that in mammal cells. We used parthenogenetically activated (PA) porcine oocytes, which can develop into blastocysts in vitro. Four targeting gRNAs targeting the exons of porcine *NLRP3*, *ROSA26*, *APP* and *GGTA1* were designed (Fig. S5a–b). In vitro-transcribed AsCpf1 mRNA and each gRNA were pooled and microinjected into the cytoplasm of one-cell stage PA porcine embryos (100 embryos for each gRNA) at the same concentration. The injected embryos were cultured 6 days post-parthenogenetic activation until blastocyst formation. The in vitro blastocyst formation rates of embryos injected with Cpf1-gRNA$^{tRNA}$ or Cpf1-gRNA were as follows: *NLRP3*: 21 and 22%; *ROSA26*: 20 and 19%, *APP*: 21, and 22%; and *GGTA1:* 23 and 21% (Fig. 2e). The blastocyst formation rate of the embryos injected with water reached 22%. The comparable blastocyst rates among the three groups suggested that AsCpf1 mRNA and gRNAs displayed no toxic effect on early porcine embryonic

development. The single blastocyst was lysed individually for genotyping analysis. DNA fragments surrounding the target site were amplified via PCR and subjected to Sanger sequencing for identification of mutations after sub-cloning into the T vector. The results showed that all four Cpf1-gRNA$^{tRNA}$ and Cpf1-gRNA can induce indel mutations at the target regions with different mutagenesis efficiencies. However, Cpf1-gRNA$^{tRNA}$ exhibited higher cleavage activity (52.40% for *NLRP3*, 80.00% for *ROSA26*, 90.50% for *APP* and 60.90% for *GGTA1*) than Cpf1-gRNA (27.30% for *NLRP3*, 57.90% for *ROSA26*, 31.80% for *APP* and 33.30% for *GGTA1*) (Fig. 2f). Taken together, those results demonstrated that the insertion of pre-tRNA in Cpf1-gRNA can improve the efficiency of CRISPR/Cpf1-mediated mammal genome editing. As a proof of concept, we applied the refined Cpf1-gRNA$^{tRNA}$ system as a gene editing tool to generate gene-modified rabbit and pig models.

## Generation of *WRN* KO rabbits using the Cpf1-gRNA$^{tRNA}$ system

Previous reports showed the successful generation of gene-edited rabbits via direct injection of the CRISPR/Cas9 system into one-cell rabbit embryos [30]. However, the performance of CRISPR/Cpf1 injection in generating of gene-modified rabbits has not been reported. Thus, we subsequently verified whether Cpf1-gRNA$^{tRNA}$ structure can be used to efficiently generate gene-modified rabbits. The endogenous gene *WRN*, which is associated with premature aging [31], was selected as a gene of interest. Two gRNAs (E4-gRNA$^{tRNA}$ and E6-gRNA$^{tRNA}$) targeting exons 4 and 6 of the rabbit *WRN* gene were designed and constructed (Fig. 3a, Fig. S6a). The in vitro-transcribed mRNAs of AsCpf1 and E6-gRNA$^{tRNA}$ only or E4-gRNA$^{tRNA}$ and E6-gRNA$^{tRNA}$ were microinjected into the cytoplasm of 60 one-cell stage rabbit embryos (30 embryos per condition). After 3.5 days of in vitro culture, the single blastocyst was harvested and lysed for genotyping analysis. With a mixture of Cpf1 mRNA and E6-gRNA$^{tRNA}$, the mutation efficiency was as high as 92.9% (Table S2) in the injected blastocysts in the intended *WRN* exon 6 locus, as determined by Sanger sequencing. The indel mutation patterns of each blastocyst ranged from 4 bp to 30 bp as determined by T-cloning and Sanger sequencing (Fig. S6b). When a mixture of Cpf1 mRNA and E4-gRNA$^{tRNA}$ and E6-gRNA$^{tRNA}$ was used, the desired large fragment deletion of *WRN* (1.8 kb deletion) was observed in blastocysts E3, E5, E6 and E11 (4/16, 25%) (Fig. S7a–d, Table S2).

To determine whether live *WRN* gene-modified rabbits can be obtained from microinjected embryos, we transferred the injected embryos into surrogate rabbits. A total of 127 embryos injected with E6-gRNA$^{tRNA}$ and AsCpf1 mRNA were transferred into four recipient rabbits. Three pregnant

**A**

E4 F · E6 F · E4 · E5 · E6 · E7

E4-gRNA · E4 R · E6-gRNA · E6 R

**B**

**C**

E6-gRNA

```
              5'-GTGCAGAGACCTGGAGCCTCAATGGTCTGGTTAAGCACCTCCTAGGTAAACAGCTTCTGAAAGA-3'   WT
201-1 ┌ 5'-GTGCAGAGACCTGGAGCCTCAA-------------C-----------AACAGCTTCTGAAAGA-3'   (Δ 25)
      └ 5'-GTGCAGAGACCTGGAGCCTC----------------------AGGTAAACAGCTTCTGAAAGA-3'   (Δ 23)
      ┌ 5'-GTGCAGAGACCTGGAGCCTCAA-----TGGTTAAGCACCTCCTAGGTAAACAGCTTCTGAAAGA-3'   (Δ 5)
201-2 ┤ 5'-GTGCAGAGACCTGGAGCCTCAA----------AAGCACCTCCTAGGTAAACAGCTTCTGAAAGA-3'   (Δ 10)
      └ 5'-GTGCAGAGACCTGGAG-----------------CCTCCTAGGTAAACAGCTTCTGAAAGA-3'   (Δ 21)
      ┌ 5'-GTGCAGAGACCTGGAGCCTCA-------------gAGGTAAACAGCTTCTGAAAGA-3'   (Δ 21, +1)
202-1 ┤ 5'-GTGCAGAGACCTGGAGCCTC---GGT----------ACCTCCTAGGTAAACAGCTTCTGAAAGA-3'   (Δ 13)
      └ 5'-GTGCAGAGACCTGGAGCCTC---------cTAAGCACCTCCTAGGTAAACAGCTTCTGAAAGA-3'   (Δ 11, +1)
      ┌ 5'-GTG-A-----------------------AAGCACCTCCTAGGTAAACAGCTTCTGAAAGA-3'   (Δ 28)
      │ 5'-GTGCAGAGACCTGGAG------------------CCTCCTAGGTAAACAGCTTCTGAAAGA-3'   (Δ 21)
202-2 ┤ 5'-GTGCAGAGACCTGGAGCCTCAATGGTC-----AAGCACCTCCTAGGTAAACAGCTTCTGAAAGA-3'   (Δ 5)
      │ 5'-GTGCAGAGACCTGGAGCCTCAATGGTCTGG-TAAGCACCTCCTAGGTAAACAGCTTCTGAAAGA-3'   (Δ 1)
      └ 5'-GTGCAGAGACCTGG------------------AGCACCTCCTAGGTAAACAGCTTCTGAAAGA-3'   (Δ 19)
202-3 ┤ 5'-GTGCAGAGACCTGGAGCCTCAATG----GGTTAAGCACCTCCTAGGTAAACAGCTTCTGAAAGA-3'   (Δ 4)
      ┌ 5'-GTGCAGAGACCTGGAG------------------CCTCCTAGGTAAACAGCTTCTGAAAGA-3'   (Δ 21)
205-1 ┤ 5'-GTGCAGAGACCTGGAGC-----------------ACCTCCTAGGTAAACAGCTTCTGAAAGA-3'   (Δ 19)
      └ 5'-GTGCAGAGACCTGGAGCCTCcA------------------GGTAAACAGCTTCTGAAAGA-3'   (Δ 23, +1)
```

**D**

**E**

301-1 301-2 302-1 302-2 302-3 302-4 305-1 305-2 305-3 305-4

E4F + E6R — 500bp

E4F + E4R — 500bp

E6F + E6R — 750bp

**F**

E4-gRNA · E6-gRNA

```
        5'GATTTGACATGGAATGGCCACCAGTGTACACTAAAGGGAAAT(1750bp)ATGGTCTGGTTAAGCACCTCCTAGGTAAAC-3'   WT
301-1 ┌ 5'G---------------------------------------------------------------------ACCTCCTAGGTAAAC-3'   (Δ 1809)
      │ 5'----------------------TACACTAAAGGGAAATCAAGTAGAGTTGCA-3'   (Δ 20)
      └         5'-AGGACCTGGAGCCT--AG--------AGCACCTCCTAGGTAAAC-3'   (Δ 12)
      ┌ 5'GATTTGACATGGA-----------------------(694 bp)ATGGTCTGGTTAAGCACCTCCTAGGTAAAC-3'   (Δ 1085)
      │ 5'GATTTGACA-------CTAGTCATGTGACACTAAAGGGAAATCAAGTAGAGTTGCA-3'   (Δ 18, +11)
301-2 ┤         5'-AGAGACCTGGAGCCTC----------AAGCACCTCCTAGGTAAAC-3'   (Δ 12)
      │         5'-AGAGACCTGG-----------------AGCACCTCCTAGGTAAAC-3'   (Δ 19)
      │         5'-AGAGACCTGGAG------------------CCTCCTAGGTAAAC-3'   (Δ 21)
      └         5'----------------------------------------3'   (Δ 347)
      ┌ 5'GATTTGACATGG----------------------------------GCACCTCCTAGGTAAAC-3'   (Δ 1793)
302-3 ┤ 5'----------------------------------------------3'   (Δ 231)
      └         5'-AGAGACCTGGAG------------------CCTCCTAGGTAAAC-3'   (Δ 21)
      ┌ 5'GATTTGACATGGAA---------------------------------ACCTCCTAGGTAAAC-3'   (Δ 1793)
      │ 5'GATTTGACATGGAA-------CAGTGTACACTAAAGGGAAATCAAGTAGAGTTGCA-3'   (Δ 7)
302-4 ┤ 5'GATTTGACATGGA-------CAGTGTACACTAAAGGGAAATCAAGTAGAGTTGCA-3'   (Δ 8)
      │         5'-AGAGACCTGGAG------------------CACCTCCTAGGTAAAC-3'   (Δ 19)
      └         5'-AGAGACCTGGAG------------------CCTCCTAGGTAAAC-3'   (Δ 21)
      ┌ 5'GATTTGACATG---------------TACACTAAAGGGAAATCAAGTAGAGTTGCA-3'   (Δ 15)
305-1 ┤         5'-AGAGACCTGGAGCCTCAAT--------AGCACCTCCTAGGTAAAC-3'   (Δ 10)
      └         5'-AGAGACCTGGAGCCTCA------------CACCTCCTAGGTAAAC-3'   (Δ 14)
      ┌ 5'GATTTGACATGGAA-------AGTGTACACTAAAGGGAAATCAAGTAGAGTTGCA-3'   (Δ 8)
      │ 5'GATTTGACA-----------------CTAAAGGGAAATCAAGTAGAGTTGCA-3'   (Δ 21)
305-2 ┤         5'-AGAGACCTGGAGCCTCAATGGT----TAAGCACCTCCTAGGTAAAC-3'   (Δ 5)
      └         5'-AGAGACCTGG-----------------AGCACCTCCTAGGTAAAC-3'   (Δ 19)
      ┌ 5'GATTTGACA-----------------CTAAAGGGAAATCAAGTAGAGTTGCA-3'   (Δ 21)
305-4 ┤         5'-AGAGACCTGGAGCCTCAA------TTAAGCACCTCCTAGGTAAAC-3'   (Δ 8)
      └         5'----------------------------------------3'   (Δ 126)
```

surrogates reached full term and gave birth to six live rabbits (three male and three female) after 30 days of gestation (Fig. 3b, Table S3). When 90 embryos were injected with E4-gRNA$^{tRNA}$, E6-gRNA$^{tRNA}$ and AsCpf1 mRNA, which were expected to generate large fragment deletion of the

WRN gene. The embryos were transferred into three recipient rabbits, and all recipient mothers were pregnant and reached full term and gave birth to 10 live pups (four male and six female) (Fig. 3d, Table S3). Genomic DNA samples from each F0-generation pup were isolated, and WRN

◀**Fig. 3** Generation of *WRN* KO rabbits using the Cpf1-gRNA^tRNA system. **a** Schematic diagram of two gRNA target sites located in exons 4 and 6 of the rabbit *WRN* locus. The gRNA target sites are indicated by black arrow. rWRN-E4F+rWRN-E4R and rWRN-E6F+rWRN-E6R primer pairs were designed to detect the mutation patterns in exons 4 and 6, respectively. rWRN-E4F and rWRN-E6R were used to detect large fragment deletion. **b** Photograph of newborn *WRN* mutant rabbits carrying indel mutations ranging from 1 to 23 bp in exon 6. **c** T vector cloning and Sanger sequencing of the targeting sites of exon 4 in all six rabbit pups, and the WT sequence is shown at the top with the target sites highlighted in red. **d** Photograph of newborn *WRN* mutant rabbits carrying large fragment deletions. **e** The mutation determination of 1.8 kb deletions of *WRN* gene in newborn rabbit pups by PCR. Gel electrophoresis photograph indicates that 301-1, 301-2, 302-3, and 302-4 rabbits contain large fragments deletion (upper). In addition, mutation patterns for each gRNA^tRNA were detected using primer pairs rWRN-E4F+rWRN-E4R and rWRN-E6F+rWRN-E6R. **f** T-cloning and Sanger sequencing of mutant alleles of *WRN* rabbits (301-1, 301-2, 302-3, and 302-4). The 301-1, 301-2, 302-3, and 302-4 founders contain 1809 bp, 1085 bp, 1793 bp and 1793 bp fragment deletions, respectively

mutations were detected via PCR and Sanger sequencing. As shown in Fig. 3c, *WRN* mutations occurred at exon 6 of all six bunnies (100%) derived from E6-gRNA^tRNA alone. Indel mutations in *WRN* ranged from 1 bp to 23 bp. Most indels exhibited mosaic with multiple mutation patterns in each individual.

For bunnies derived from the combination of E4 and E6, as shown in Fig. 3e and f, the desired 1.8-kb large fragment deletion of *WRN* was identified in pups 301-1, 301-2, 302-3, and 302-4. The mutation efficiency of the CRISPR/Cpf1 system for each gRNA^tRNA was also determined by T-cloning and Sanger sequencing. PCR primers rWRN-E4F and rWRN-E4R were used for the detection of mutations with E4-gRNA^tRNA, whereas rWRN-E6F and rWRN-E6R were used for E6-gRNA^tRNA. The T-cloning and Sanger sequencing results demonstrated that 301-1, 301-2, 302-3, 302-4, 305-1, 305-2, and 305-4 had indel mutations in exons 4 and 6 ranging from 5 bp to 347 bp (Fig. 3g, h). Furthermore, DNA waveform data indicated that 7 of the 10 pups manifested biallelic mutations at the target sites of exons 4 and 6. These results demonstrated that Cpf1-gRNA^tRNA structure can induce indels via single gRNA injection or large fragment deletion via dual gRNA injection.

## Generation of *DMD* KO and *PLN^R14del* pigs via CRISPR/Cpf1-mediated gene editing and SCNT

For the *DMD* gene, Cpf1-gRNA^tRNA was designed to target exon 61, which is a frequent mutation location in human DMD patients (Fig. S8a) [32]. To introduce the orthologous *PLN^R14del* mutation into the porcine genome, a point mutation strategy was employed [25]. Phospholamban (*PLN*)-Cpf1-gRNA^tRNA targeting the region and overlapping with the intended mutation was designed. ssODN^R14del with a

length of 89 nt, containing a 40-nt right arm and a 43-nt left arm, was used as a homology-directed repair (HDR) donor (Fig. S8b). The synthesized ssODN templates harbored a three-base (AGA) deletion. As a result, pathogenic mutation of dilated cardiomyopathy (DCM) *PLN^R14del* will be induced at position R14 of the porcine *PLN* gene. In addition, two silent mutations (GC**TT**CA > GC**G**TC**G**) on the targeting site were introduced to generate a new SalI restriction enzyme site (**TT**CA**A**C > **G**TC**G**AC), which facilitates genotype identification of the targeted colonies and avoids repetitive digestion.

To validate the targeting activity of Cpf1 and *DMD*/*PLN*-gRNA^tRNA in porcine genome, the in vitro-transcribed AsCpf1 mRNA (50 ng/μL) and gRNAs^tRNA (20 ng/μL) were microinjected into the cytoplasm of one-cell stage PA porcine embryos. For *PLN^R14del*, to induce point mutations, HDR donor, ssODN^R14del (5 ng/μL), was also injected to the cytoplasm of the embryos. The injected parthenogenetic embryos were cultured until the blastocyst stage. A single blastocyst was individually lysed for genotyping analysis. As summarized in Table S2, the designed gRNAs for both the *DMD* and *PLN* genes can generate mutants in embryos at high efficiencies (66.7% for *DMD* and 78.5% for *PLN*). Specifically, for *PLN*-gRNA^tRNA, among the 107 PA embryos analyzed, 21 (19.6%) exhibited the intended point mutation (Fig. S8b). The above results showed that the Cpf1-gRNA^tRNA system not only can be used to generate KO mutations with high efficiency, but also can introduce intended precise point mutations into target sites with the help of HDR donors in the porcine genome, indicating that the designed gRNA^tRNA and ssODNs did work with the Cpf1 protein. Thus, *DMD*-gRNA^RNA and *PLN*-gRNA^tRNA were used to construct pig models through a combination of somatic cell gene targeting with SCNT in the following experiments.

Primary PFFs isolated from a 35-day-old fetus of a Bama mini-pig were used to prepare gene-targeting cells for nuclear transfer. To target the *DMD* gene, we co-transfected AsCpf1, *DMD*-gRNA^tRNA expressing vectors into PFFs by electroporation. To induce the *PLN^R14del* mutation, we co-transfected AsCpf1, *PLN*-gRNA^tRNA vectors and ssODN^R14del into PFFs. After treatment with G418 for approximately 10 days, the surviving cell colonies were collected and then analyzed individually. For the *DMD* gene, the mutation rate among the selected cell colonies at the target loci totaled 41.8% (28/67) as analyzed by direct sequencing of PCR products covering the target locus (Fig. S9a, Table S4, Table S5). For the *PLN* gene, PCR products covering the target locus were first digested by SalI. Among the 103 colonies, two cells with the *PLN^R14del* mutation were identified; one contained an allele with a point mutation and one allele 8 bp deletion, and the other featured biallelic point mutations (Fig. S9b, Table S6). Sequencing results further

confirmed that the two selected colonies were correctly targeted with three-base (AGA) deletions and two silent mutations (GCTTCA > GCGTCG) (Fig. S9c-9d). In addition, NHEJ was also observed in many colonies generated by Cpf1-gRNA$^{tRNA}$ and ssODNs (55/103, 54.4%) (Table S6).

Six $DMD^{-/-}$ cell colonies and two $PLN^{R14del}$ cell colonies were used as donors for SCNT. We usually pooled 2–6 colonies in one nuclear transfer, and the reconstructed embryos from pooled cells were transferred to a surrogate. A total of 1776 reconstructed embryos derived from $DMD^{-/-}$ cells were generated and transferred into eight

surrogate mothers. Among these surrogate mothers, four surrogates were confirmed pregnant through ultrasound examination at 1 month post-transfer. These pregnant surrogates all developed to term and gave birth to eight male-cloned piglets (Fig. 4a, Table S7). Among the eight piglets, four were weak at birth and died in 2 weeks. The remaining piglets grew to adult age. DNA sequencing analysis results revealed that all these newborns carried the expected homozygous mutations at the target loci (Fig. 4b, Fig. S10a). This finding is consistent with the genotype of the donor cells.
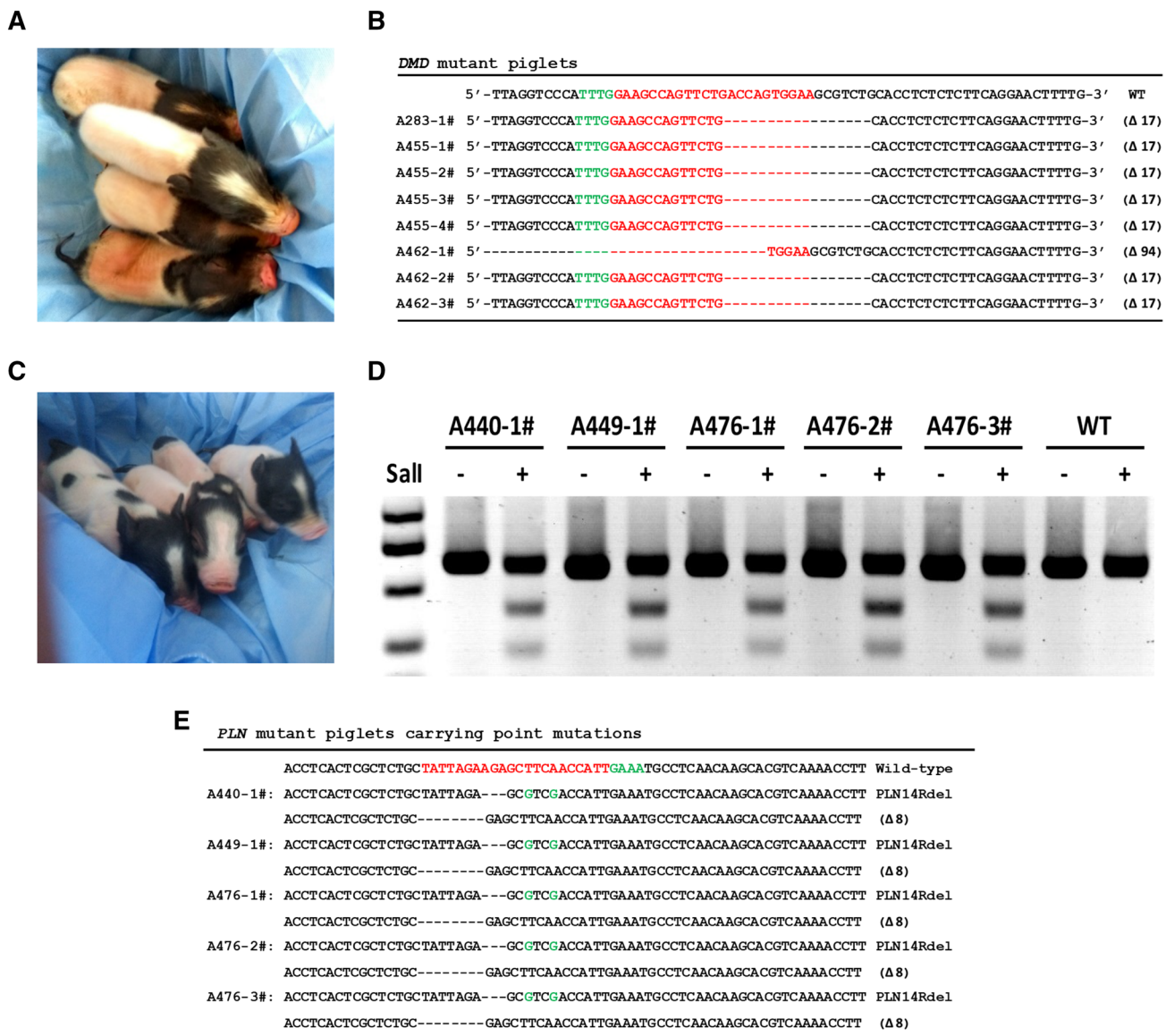


**Fig. 4** Generation of *DMD* KO and *PLN*$^{R14del}$ pigs via CRISPR/Cpf1-mediated gene editing and SCNT. **a** Photograph of newborn *DMD* KO cloned piglets. **b** All *DMD* KO cloned piglets were genotyped by Sanger sequencing. **c** Photograph of newborn *PLN*$^{R14del}$ cloned piglets. **d** Identification of newborn *PLN*$^{R14del}$ piglets by PCR-Sal I digestion. The two small DNA fragments digested by Sal I restriction enzyme indicate the ssODN-mediated point mutation occurred at the target site. **e** All *PLN*$^{R14del}$ piglets were genotyped by Sanger sequencing

A total of 1757 reconstructed embryos derived from *PLN^R14del* cells were introduced into seven surrogates. Three pregnant recipients developed to term and eventually gave birth to five cloned piglets (Fig. 4c, Table S7). Among these five piglets, one was stillborn and two were weak at birth and died after 2 weeks. The remaining piglet was born normal but also died 3 months after birth. Genomic DNA was extracted from the ear tissues of these piglets and genotyped through PCR and Sal I digestion (Fig. 4d). All five piglets were cloned from 98# cell colony and were heterozygous for the intended mutations. Sequencing results further confirmed the desired precise modification in *PLN* in the cloned piglets (Fig. 4e, Fig. S10b).

We further examined whether *DMD* mutations would result in dystrophin dysfunction and induce the related phenotypes characterized by muscle degeneration due to lack of dystrophin. The *DMD* KO pigs showed muscle weakness, which was reflected in their movement (Movie S1). We first investigated dystrophin expression in the skeletal and smooth muscle of the targeted pig and compared it with the expression in muscles from WT pigs of the same age. Western blot and immunostaining with an antibody for dystrophin indicated that the dystrophin in the biceps femoris muscle, heart, and diaphragm muscle of *DMD* KO piglets completely disappeared compared with that of WT (Fig. 5c, e). Then, we investigated the pathologies of the *DMD*-modified pig. Hematoxylin and eosin (H&E) staining also revealed extensive disruption of muscle structure, including disordered myofibers in skeletal muscle tissues (Fig. 5a). In addition, muscle cell nuclei were often aggregated due to necrosis of the muscle fibers. Multifocal areas of pale discoloration in cardiac muscles in the founder were also observed. For *PLN^R14del* piglets, whole mRNA was extracted from the heart of dead piglets and age-matched WT piglets. *PLN*-mRNA was amplified through reverse-transcription PCR (RT-PCR) and sequencing. As shown in Fig. 5d, the *PLN^R14del* piglets contained AGA deletion mRNA. Heart H&E staining results of *PLN^R14del* piglets showed no significant differences in tissue morphology or cell shape and size, probably because the pigs were too young to show mutation effects. This finding matches the phenotype in the early stage of *PLN^R14del* patients and *PLN^R14del* transgenic mice (Fig. 5b) [33]. In this study, typical DCM symptoms, such as shaking, rigidity, slowness of movement, and difficulty walking, were not observed in 3-month-old live mutant pigs.

## Off-target analysis of gene-modified rabbits and pigs

To test whether off-targeting occurred in these genetically modified rabbits and piglets, we screened the rabbit or pig genome using Cas-OFFinder (http://www.rgenome.net/cas-offinder/) [29] and predicted 4, 1, 3, and 7 potential off-target sites with 3–5 bp mismatches for WRN-E4-gRNA^tRNA, WRN-E6-gRNA^tRNA, DMD-gRNA^tRNA, and PLN-gRNA^tRNA target sites, respectively (Fig. 6a–c). We amplified these off-target sites from all newborn rabbits and cloned piglets by PCR and analyzed them using deep sequencing. More than 99.9% of the amplicons of possible off-target sites comprised WT sequences. The remaining 0.1% consisted of a small number of amplicons (< 0.1%) carrying different sequences (Fig. 6a–c). These amplicons were also detected when we analyzed WT rabbits and piglets, indicating that these sequence changes may be introduced by PCR errors or sequence errors. These results indicated that genome editing occurred in only the targeted regions and no off-target mutations were introduced at other untargeted sites.

## Discussion

The reported genome editing efficiency of CRISPR/Cpf1 was ultimately lower than that of SpCas9 regardless in human cells or in mouse embryos. So far, the potential of Cpf1 for targeted mutagenesis has not been successfully validated in mammals other than human cells and mouse embryos. Our initial attempts to achieve gene-edited rabbits and pigs with the conventional CRISPR/Cpf1 system (data not shown) were unsuccessful. To address these issues, we refined the Cpf1-gRNA system with pre-tRNA, established a gRNA^tRNA system for Cpf1 which remarkably enhance the gene editing efficiency in mammalian cell lines and embryos. In addition, using this system, we successfully generated gene-edited pigs and rabbits with high efficiency.

Previous study showed that Cas9 gRNA flanked with rice pre-tRNA^Gly can permit highly efficient multiplex gene disruption by Cas9 in rice [34], *Drosophila* [12], maize [35], and yeast [36]. Initially, we attempted to construct multiple gRNA expression vectors flanked with tRNA^Gly for Cpf1 under the control of a single Pol III promoter in human cell lines. However, the in vitro results showed that only the first gRNA functioned well, whereas later developed gRNA failed to function properly (date not shown). This finding was consistent with the results previously reported in rice [37] and *Drosophila* [12]. The causes of these observations remain unknown. Unexpectedly, we observed that insertion of a pre-tRNA into the gRNA for Cpf1 was able to improve single target editing efficiency, especially, when in vitro-transcribed Cpf1 mRNA and gRNA^tRNA were applied for gene editing in the embryos. This phenomenon may be tentatively explained as follows.

Compared with gRNA components and the structure of Cas9, that of Cpf1 holds three different features. First, the 3′-5′ end of the gRNA for Cas9 is highly structured, and it is also the region recognized by Apo-Cas9 to form Cas9–RNA
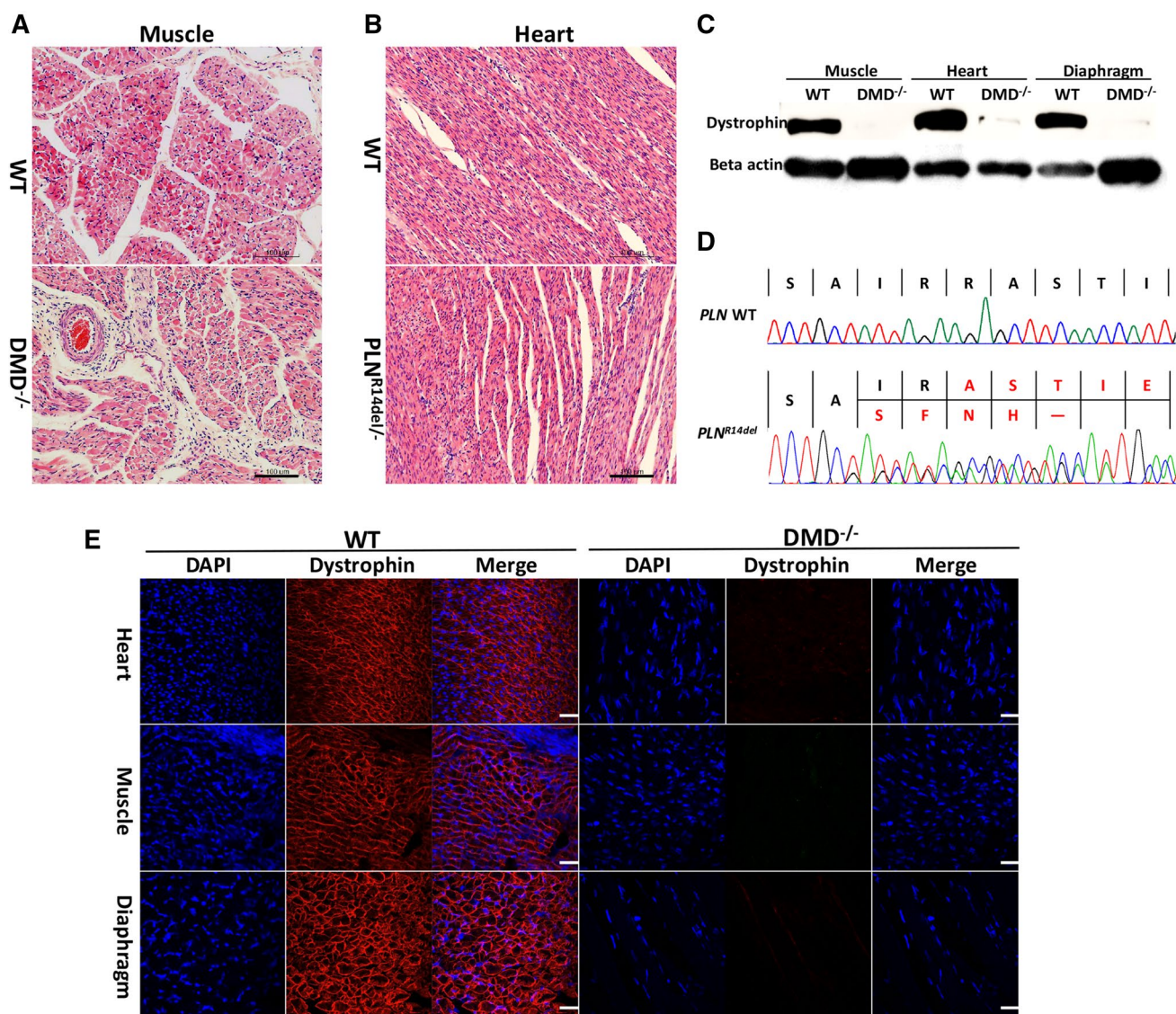
**Fig. 5** Pathological and histological alterations in *DMD* KO and *PLN^R14del* pigs. **a** and **b** H&E staining analysis of *DMD* KO and *PLN^R14del* pigs. Scale bar = 20 μm. **c** Western blot detected dystrophin expression in muscles, hearts, and diaphragms of WT and *DMD* KO pigs. **d** Sanger sequencing of RT-PCR products showed deletion of arginine (AGA) and two silent mutations in the heart of *PLN^R14del* pigs. **e** Dystrophin immunofluorescence staining showed dystrophin expression on cell membranes of WT pigs (left) in tibialis anterior muscles, cardiomyocytes, and diaphragms, but not in *DMD* KO pigs (right). Myonuclei were stained with DAPI. Scale bar = 20 μm

complex. The highly structured nature and tight binding by Cas9 likely prevent the degradation of gRNA. While the gRNA for Cpf1 may be more easily degenerated by 3′-to-5′ exonucleases due to the less structured. Second, the previous study indicated that the $K_d$ values of the Cpf1 and gRNA interaction are much higher than those of the Cas9 interaction (~16 nM for AsCpf1 and ~10 pM for Cas9) [38]. The higher $K_d$ values for Cpf1 might mean that the canonical gRNA for Cpf1 is more prone to dissociation from Cpf1 enzymes, which would then be exposed to nucleases for degradation. Third, the gRNA for Cpf1 only comprises crRNA, not tracrRNA [6]. Notably, instead of being located upstream

as in Cas9 [39], the sequence complementary to the protospace of Cpf1 is downstream of crRNA, thus enabling direct exposure of sequence complementary to the protospace to 3′-to-5′ exonucleases. Those features illuminated that the limited efficiency of Cpf1 system might own to the rapid degradability of gRNA.

As a foreign RNA, the injected gRNA in Cpf1 system is more sensitive to 3′-to-5′ exonuclease than that in Cas9 system. When gRNA^tRNA was applied, the gRNA had to be split off of the precursor by RNAses first. In vitro experiment showed the process of pre-tRNA in 3 h [40]. Therefore, the extra gRNA-releasing process may delay the digestion of
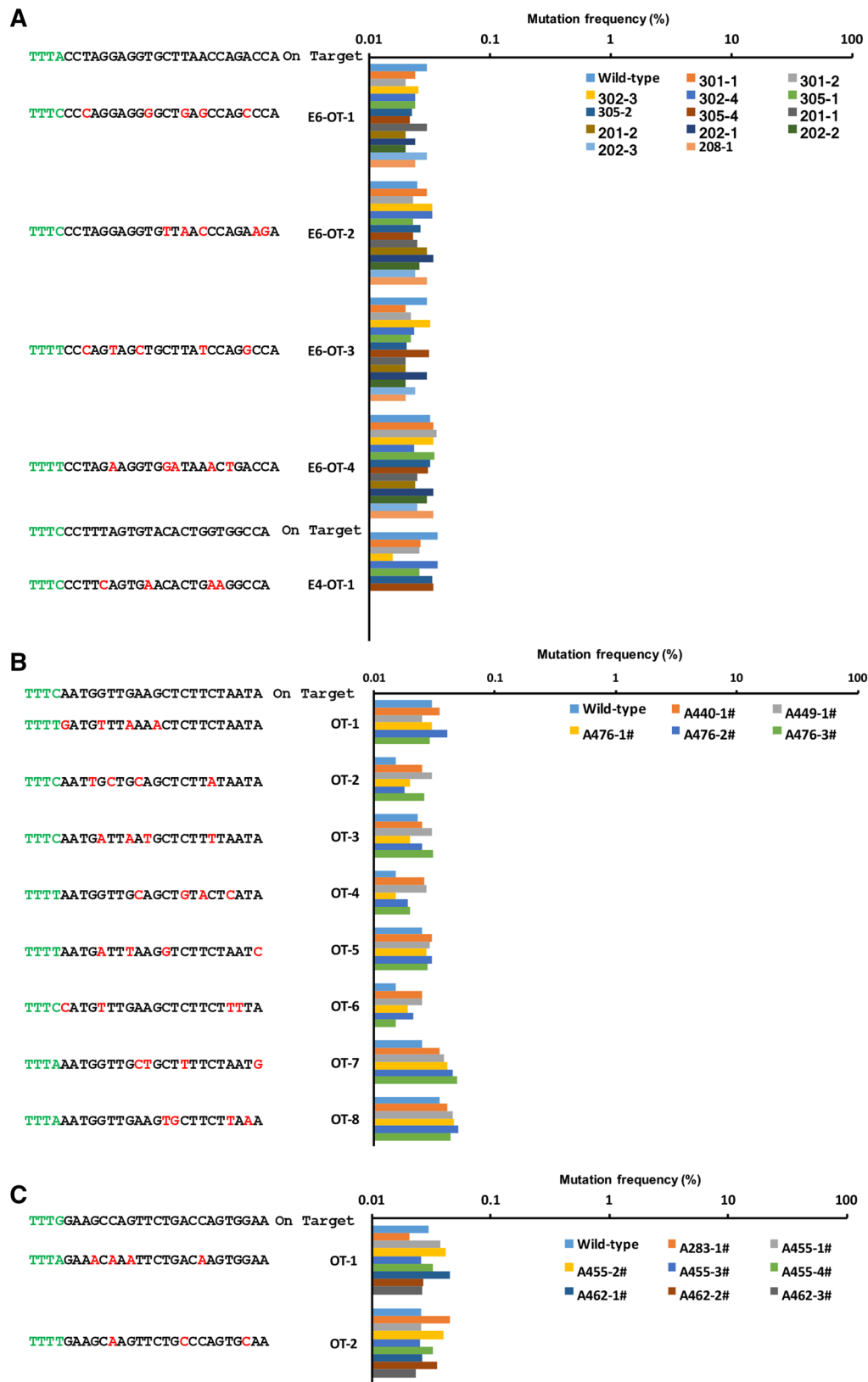
**Fig. 6** Off-target analysis of mutant rabbits and pigs mediated by Cpf1-gRNA$^{tRNA}$ system. Off-target analysis of predicted potential off-target sites with 3–5 bp mismatches for WRN-E4-gRNA$^{tRNA}$ (**a**), WRN-E6-gRNA$^{tRNA}$ (**a**), DMD-gRNA$^{tRNA}$ (**c**), and PLN-gRNA$^{tRNA}$ (**b**) target sites. The potential off-target sites were amplified by PCR from a genomic DNA sample of a WT and gene-modified rabbits and pigs, and analyzed by deep sequencing. Mismatched bases are labeled in red, and PAM sites were labeled in green

3′-to-5′ exonucleases, synchronizing the function of Cpf1 protein and gRNA. Consequently, the addition of a pre-tRNA sequence under sequence complementary to the proto-space could protect it from immediate digestion by 3′-to-5′ exonucleases [41] and increase the gene editing efficiency of the Cpf1-gRNA system.

tRNA is one of the most abundant RNA in organisms. A total of 597 predicted pre-tRNA genes have been found in the human genome which transcribes 61 kinds of tRNA encoding 20 different amino acids. Each pre-tRNA contains different 5′ leader and 3′ trailer sequences, which are associated with the cleavage efficiency of endogenous tRNA processing efficiency [41]. The use of different pre-tRNA may lead to different gene editing efficiencies. Using the HEK293-*hROSA26*-EGFP reporter cell line, we investigated the effects of different human pre-tRNAs. We found that 43 different EGFP-gRNA$^{tRNA}$ presented diverse EGFP disruption ratios ranging from 30.40 to 59.37%. Many EGFP-gRNA$^{tRNA}$ were significantly better than the original gRNA for Cpf1. tRNA$^{Gln-TTG-1-1}$ showed the best gene editing efficiency (60%), which was comparable to that of the CRISPR/Cas9 control (67%). Similar to its enhancement of targeting efficiency in mammalian cells, the gRNA$^{tRNA}$ system can also enhance the targeting efficiency in mammalian embryos.

To achieve the transcription of gRNA, we used U6 and T7 promoters to drive the gRNA, and a 5′ G is a requirement for the efficient transcription of gRNA in vitro. A recent pre-print showed that this 5′ G may have significant deleterious effects on Cpf1-gRNA activity [42]. If chemical synthesis approach is used instead of in vitro transcription to achieve gRNA$^{tRNA}$ without a 5′ G, the gene editing efficiency with our gRNA$^{tRNA}$ system may reach a higher level.

Many of the resulting founder animals obtained through co-injection of Cpf1 mRNA and gRNA into one-cell stage embryos can be chimeric with multiple mutations. To establish animals with a single mutation, one or two rounds of further breeding and selection must be performed among the offspring. However, this procedure is not easily applied in large animals, such as pigs, because these animals feature long gestation cycles and the process entails high recipient costs. To address this issue, gene-targeted somatic cells can be used as a donor for SCNT to produce gene-targeted animals with identical mutations. Thus, we investigated the feasibility of generating gene-targeted pigs by targeting genes in somatic cells via the Cpf1-gRNA$^{tRNA}$ system with a SCNT approach. Genetically modified pigs have been considered to be ideal models for mimicking human diseases [43]. We successfully developed pig models for human DMD disease and DCM disease (*PLNR$^{14del}$*) via combining gRNA$^{tRNA}$ system-mediated gene-edited somatic cells and a nuclear transfer approach. The ratio of the selected cell colonies with knockout of the *DMD* gene (41.8%) and with point mutation of the *PLN* gene (2%) in primary porcine fibroblasts and the pig cloning efficiency with gene-edited cells were comparable to those of the Cas9-gRNA system [25]. The results demonstrated that precise gene mutations, including knockouts and point mutations, can be effectively achieved using the gRNA$^{tRNA}$ system combined with SCNT without mosaic mutations.

In summary, our refined Cpf1-gRNA$^{tRNA}$ system is able to efficiently induce a variety of mutation patterns, including indels, large fragment deletions and precise point mutations, in mammalian systems. This study is the first to generate gene-edited large animals by CRISPR/Cpf1 through embryo injection and SCNT. The system established in this study can act as an effective genome editing tool in mammalian systems for research applications and therapeutics.

## Compliance with ethical standards

**Conflict of interest** The authors declare that they have no conflict of interest.

## References

1. Mali P, Esvelt KM, Church GM (2013) Cas9 as a versatile tool for engineering biology. Nat Methods 10(10):957–963
2. Cho SW, Kim S, Kim JM, Kim J-S (2013) Targeted genome engineering in human cells with the Cas9 RNA-guided endonuclease. Nat Biotechnol 31(3):230–232
3. Jinek M, Chylinski K, Fonfara I, Hauer M, Doudna JA, Charpentier E (2012) A programmable dual-RNA-guided DNA endonuclease in adaptive bacterial immunity. Science 337(6096):816–821
4. Kleinstiver BP, Prew MS, Tsai SQ, Topkar VV, Nguyen NT, Zheng Z, Gonzales APW, Li Z, Peterson RT, Yeh J-RJ et al (2015) Engineered CRISPR-Cas9 nucleases with altered PAM specificities. Nature 523(7561):481
5. Hu JH, Miller SM, Geurts MH, Tang W, Chen L, Sun N, Zeina CM, Gao X, Rees HA, Lin Z et al (2018) Evolved Cas9 variants with broad PAM compatibility and high DNA specificity. Nature 556:57–63
6. Zetsche B, Gootenberg JS, Abudayyeh OO, Slaymaker IM, Makarova KS, Essletzbichler P, Volz SE, Joung J, van der Oost J, Regev A et al (2015) Cpf1 is a single RNA-guided endonuclease of a class 2 CRISPR-Cas system. Cell 163(3):759–771
7. Endo A, Masafumi M, Kaya H, Toki S (2016) Efficient targeted mutagenesis of rice and tobacco genomes using Cpf1 from Francisella novicida. Sci Reports 6:38169

8. Xu R, Qin R, Li H, Li D, Li L, Wei P, Yang J (2017) Generation of targeted mutant rice using a CRISPR-Cpf1 system. Plant Biotechnol J 15(6):713–717

9. Tang X, Lowder LG, Zhang T, Malzahn AA, Zheng X, Voytas DF, Zhong Z, Chen Y, Ren Q, Li Q et al (2017) A CRISPR-Cpf1 system for efficient genome editing and transcriptional repression in plants. Nature plants 3:17018

10. Kim H, Kim ST, Ryu J, Kang BC, Kim JS, Kim SG (2017) CRISPR/Cpf1-mediated DNA-free plant genome editing. Nature Commun 8:7

11. Ungerer J, Pakrasi HB (2016) Cpf1 is a versatile tool for CRISPR genome editing across diverse species of cyanobacteria. Sci Reports 6:39681

12. Port F, Bullock SL (2016) Augmenting CRISPR applications in drosophila with tRNA-flanked sgRNAs. Nat Methods 13(10):852–854

13. Hur JK, Kim K, Been KW, Baek G, Ye S, Hur JW, Ryu SM, Lee YS, Kim JS (2016) Targeted mutagenesis in mice by electroporation of Cpf1 ribonucleoproteins. Nat Biotechnol 34(8):807–808

14. Kim Y, Cheong SA, Lee JG, Lee SW, Lee MS, Baek IJ, Sung YH (2016) Generation of knockout mice by Cpf1-mediated gene targeting. Nat Biotechnol 34(8):808–810

15. Watkins-Chow DE, Varshney GK, Garrett LJ, Chen Z, Jimenez EA, Rivas C, Bishop KS, Sood R, Harper UL, Pavan WJ et al (2017) Highly efficient Cpf1-mediated gene targeting in mice following high concentration pronuclear injection. G3 7(2):719–722

16. Zetsche B, Heidenreich M, Mohanraju P, Fedorova I, Kneppers J, DeGennaro EM, Winblad N, Choudhury SR, Abudayyeh OO, Gootenberg JS et al (2017) Multiplex gene editing by CRISPR-Cpf1 using a single crRNA array. Nat Biotechnol 35(1):31–34

17. Zhang Y, Long C, Li H, McAnally JR, Baskin KK, Shelton JM, Bassel-Duby R, Olson EN (2017) CRISPR-Cpf1 correction of muscular dystrophy mutations in human cardiomyocytes and mice. Sci Adv 3(4):e1602814–e1602814

18. Kleinstiver BP, Tsai SQ, Prew MS, Nguyen NT, Welch MM, Lopez JM, McCaw ZR, Aryee MJ, Joung JK (2016) Genome-wide specificities of CRISPR-Cas Cpf1 nucleases in human cells. Nat Biotechnol 34(8):869–874

19. Kim D, Kim J, Hur JK, Been KW, Yoon SH, Kim JS (2016) Genome-wide analysis reveals specificities of Cpf1 endonucleases in human cells. Nat Biotechnol 34(8):863–868

20. Yang M, Wei H, Wang Y, Deng J, Tang Y, Zhou L, Guo G, Tong A (2017) Targeted disruption of V600E-mutant BRAF gene by CRISPR-Cpf1. Mol Ther Nucleic Acids 8:450–458

21. Tu M, Lin L, Cheng Y, He X, Sun H, Xie H, Fu J, Liu C, Li J, Chen D et al (2017) A 'new lease of life': FnCpf1 possesses DNA cleavage activity for genome editing in human cells. Nucleic Acids Res 45(19):11295–11304

22. Lei C, Li SY, Liu JK, Zheng X, Zhao GP, Wang J (2017) The CCTL (Cpf1-assisted Cutting and Taq DNA ligase-assisted Ligation) method for efficient editing of large DNA constructs in vitro. Nucleic Acids Res 45(9):e74

23. Orlando SJ, Santiago Y, DeKelver RC, Freyvert Y, Boydston EA, Moehle EA, Choi VM, Gopalan SM, Lou JF, Li J (2010) Zinc-finger nuclease-driven targeted integration into mammalian genomes using donors with limited chromosomal homology. Nucleic Acids Res 38(15):e152–e152

24. Song J, Zhong J, Guo XG, Chen YQ, Zou QJ, Huang J, Li XP, Zhang QJ, Jiang ZW, Tang CC et al (2013) Generation of RAG 1-and 2-deficient rabbits by embryo microinjection of TALENs. Cell Res 23(8):1059–1062

25. Yang Y, Wang K, Wu H, Jin Q, Ruan D, Ouyang Z, Zhao B, Liu Z, Zhao Y, Zhang Q (2016) Genetically humanized pigs exclusively expressing human insulin are generated through custom endonuclease-mediated seamless engineering. J Molecular Cell Biol 8(2):174–177

26. Zhou X, Xin J, Fan N, Zou Q, Huang J, Ouyang Z, Zhao Y, Zhao B, Liu Z, Lai S (2015) Generation of CRISPR/Cas9-mediated gene-targeted pigs via somatic cell nuclear transfer. Cell Mol Life Sci 72(6):1175–1184

27. Xin JG, Yang HQ, Fan NN, Zhao BT, Ouyang Z, Liu ZM, Zhao Y, Li XP, Song J, Yang Y et al (2013) Highly efficient generation of GGTA1 biallelic knockout inbred mini-pigs with TALENS. PLoS One 8(12):9

28. Xin J, Yang H, Fan N, Zhao B, Ouyang Z, Liu Z, Zhao Y, Li X, Song J, Yang Y (2013) Highly efficient generation of GGTA1 biallelic knockout inbred mini-pigs with TALENS. PLoS One 8(12):e84250

29. Bae S, Park J, Kim JS (2014) Cas-OFFinder: a fast and versatile algorithm that searches for potential off-target sites of Cas9 RNA-guided endonucleases. Bioinformatics 30(10):1473–1475

30. Yang D, Xu J, Zhu T, Fan J, Lai L, Zhang J, Chen YE (2014) Effective gene targeting in rabbits using RNA-guided Cas9 nucleases. J Molecular Cell Biol 6(1):97–99

31. Zhang W, Li J, Suzuki K, Qu J, Wang P, Zhou J, Liu X, Ren R, Xu X, Ocampo A (2015) A Werner syndrome stem cell model unveils heterochromatin alterations as a driver of human aging. Science 348(6239):1160–1163

32. Koenig M, Beggs AH, Moyer M, Scherpf S, Heindrich K, Bettecken T, Meng G, Muller CR, Lindlof M, Kaariainen H et al (1989) The molecular-basis for duchenne versus becker muscular-dystrophy—correlation of severity with type of deletion. Am J Hum Genet 45(4):498–506

33. Haghighi K, Kolokathis F, Gramolini AO, Waggoner JR, Pater L, Lynch RA, Fan GC, Tsiapras D, Parekh RR, Dorn GW et al (2006) A mutation in the human phospholamban gene, deleting arginine 14, results in lethal, hereditary cardiomyopathy. Proc Natl Acad Sci USA 103(5):1388–1393

34. Xie K, Minkenberg B, Yang Y (2015) Boosting CRISPR/Cas9 multiplex editing capability with the endogenous tRNA-processing system. Proc Natl Acad Sci USA 112(11):3570–3575

35. Qi WW, Zhu T, Tian ZR, Li CB, Zhang W, Song RT (2016) High-efficiency CRISPR/Cas9 multiplex gene editing using the glycine tRNA-processing system-based strategy in maize. BMC Biotechnol 16(1):58

36. Numamoto M, Maekawa H, Kaneko Y (2017) Efficient genome editing by CRISPR/Cas9 with a tRNA-sgRNA fusion in the methylotrophic yeast Ogataea polymorpha. J Biosci Bioeng 124(5):487–492

37. Hu X, Wang C, Liu Q, Fu Y, Wang K (2017) Targeted mutagenesis in rice using CRISPR-Cpf1 system. J Genet Genom =Yi chuan xue bao 44(1):71–73

38. Yamano T, Nishimasu H, Zetsche B, Hirano H, Slaymaker IM, Li Y, Fedorova I, Nakane T, Makarova KS, Koonin EV et al (2016) Crystal structure of Cpf1 in complex with guide RNA and target DNA. Cell 165(4):949–962

39. Mali P, Esvelt KM, Church GM (2013) Cas9 as a versatile tool for engineering biology. Nat Methods 10(10):957

40. Frendewey D, Dingermann T, Cooley L, Söll D (1985) Processing of precursor tRNAs in Drosophila. Processing of the 3′end involves an endonucleolytic cleavage and occurs after 5′end maturation. J Biol Chem 260(1):449–454

41. Ibrahim H, Wilusz J, Wilusz CJ (2008) RNA recognition by 3′-to-5′ exonucleases: the substrate perspective. Biochem Biophys Acta 1779(4):256–265

42. Singh D, Mallon J, Poddar A, Wang Y, Tipanna R, Yang O, Bailey S, Ha T (2017) Real-time observation of DNA target interrogation and product release by the RNA-guided endonuclease CRISPR Cpf1. https://doi.org/10.1101/205575

43. Fan NN, Lai LX (2013) Genetically modified pig models for human diseases. J Genet Genom 40(2):67–73